

Polarity formation in crystals with long range molecular interactions: A Monte Carlo study

Luigi Cannavacciuolo and Jürg Hulliger

Citation: *The Journal of Chemical Physics* **145**, 124502 (2016); doi: 10.1063/1.4962744

View online: <http://dx.doi.org/10.1063/1.4962744>

View Table of Contents: <http://scitation.aip.org/content/aip/journal/jcp/145/12?ver=pdfcov>

Published by the [AIP Publishing](#)

Articles you may be interested in

Analysis of long-range interaction effects on phase transitions in two-step spin-crossover chains by using Ising-type systems and Monte Carlo entropic sampling technique

J. Appl. Phys. **112**, 074906 (2012); 10.1063/1.4756994

Short- and long-range orders in Fe–Cr: A Monte Carlo study

J. Appl. Phys. **106**, 104906 (2009); 10.1063/1.3257232

A Monte Carlo study of metastable structures of the cyanoadamantane crystal

J. Chem. Phys. **109**, 6753 (1998); 10.1063/1.477321

Studies of epitaxial Fe 0.5 Pd 0.5 thin films by x-ray diffraction and polarized fluorescence absorption spectroscopy

J. Appl. Phys. **84**, 2316 (1998); 10.1063/1.368298

Monte Carlo simulations of the interlamellar spacing in model n -alkane crystals

J. Chem. Phys. **108**, 2622 (1998); 10.1063/1.475648



NEW Special Topic Sections

NOW ONLINE
Lithium Niobate Properties and Applications:
Reviews of Emerging Trends

AIP Applied Physics Reviews

Polarity formation in crystals with long range molecular interactions: A Monte Carlo study

Luigi Cannavacciuolo and Jürg Hulliger^{a)}

Department of Chemistry, University of Bern, Bern, Switzerland

(Received 4 June 2016; accepted 1 September 2016; published online 22 September 2016)

Stochastic formation of a bi-polar state in three dimensional arrays of polar molecules with full Coulomb interactions is reproduced by Monte Carlo simulation. The size of the system is comparable to that of a real crystal seed. The spatial decay of the average order parameter is significantly slowed down by the long range interactions and the exact representation of correlation effects in terms of a single characteristic length becomes impossible. Finite size effects and possible scale invariance symmetry of the order parameter are extensively discussed. *Published by AIP Publishing*. [<http://dx.doi.org/10.1063/1.4962744>]

I. INTRODUCTION

The theme *statistical state of a small assembly of polar molecules*, i.e., an object emerging from a nucleation process, is of interest in view of its polarity distribution. Because of its dynamic flexibility such a seed may accommodate a statistical state showing also 180° orientational disorder of dipolar entities. The nature of the polar state resulting from this *orientational disorder* is of fundamental importance and is the object of the present work.

Model calculation based on nearest neighbor interactions of molecules has revealed a so-called bi-polar state. This means that such an assembly of molecules, having one degree of orientational freedom only, shows a statistical ground state with zero average polarization. The object splits into two domains with opposite polarization (see Fig. 1). It turns out that this state, providing no overall polarity, is for fundamental reasons¹ the “true” state.

In the present work, we perform Monte Carlo simulations of “real” molecules forming such aggregates by taking into account full electrostatic interactions between all entities. We assume a general packing similar to known crystal structures of such A- π -D (A: acceptor group, D: donor group, π : conjugated linker) type molecules comprising of interacting chains, as found in real structures. The molecule of choice is 4-bromo-2,3,5,6-tetrafluorobenzonitrile (BTFBN). This is a polar, planar molecule showing the typical A-D charge transfer outlined above, and intermolecular interactions as found in many other molecular crystals.

The extensive MC calculations confirm indeed the generally expected bi-polar state of nanosized objects with 180° orientational disorder.

II. MODEL

The model consists of a cubic $N_y \times N_z$ array of one-dimensional chains of molecules arranged in N_z layers orthogonal to the z-axis. Each layer is located at a distance d_z

from the next one and contains N_y parallel chains separated by a distance d_y . These, in turn, comprise N_x molecules longitudinally aligned along the x direction at distance d_x . Periodic boundary conditions (PBCs) are imposed on the y and z directions whereas free boundary conditions (FBCs) are left on the x.

Any couple of atoms is assumed to interact through a full Coulomb potential. In this way, the long range r^{-1} character of the interaction is carried out through the whole system and its periodic replicas. Other inter-molecular forces are included by the Lennard-Jones 12-6 potential with a cutoff radius of 2.5 times the largest atom size. The total energy of the main simulation cell reads

$$U_0 = \sum_{i < j}^N \left\{ k_C \frac{q_i q_j}{|\mathbf{r}_i - \mathbf{r}_j|} + 4\epsilon_{i,j} \left[\left(\frac{\sigma_{ij}}{|\mathbf{r}_i - \mathbf{r}_j|} \right)^{12} - \left(\frac{\sigma_{ij}}{|\mathbf{r}_i - \mathbf{r}_j|} \right)^6 \right] \right\}, \quad (1)$$

where k_C is the Coulomb constant whose value depends on the units employed, q_i is the partial charge associated to atom i previously calculated by the Gaussian 09 software²

$$\sigma_{i,j} = (\sigma_i + \sigma_j)/2 \quad \epsilon_{i,j} = \sqrt{(\epsilon_i \epsilon_j)}, \quad (2)$$

with σ_i ³ and ϵ_i ⁴ the Lennard-Jones parameters of atom i . At distances larger than the cutoff, the Lennard-Jones energy is surely negligible, being only about 2% $\epsilon_{i,j}$ and about 0.01% of the electrostatic contribution due to all interactions. The parameters in the energy Eq. (1) have been chosen to mimic the interactions of the BTFBN molecule. This is a planar polar molecule belonging to the C_{2v} point group. Based on theoretical prediction, a transition into a bi-polar state should be expected.⁵ The molecules are overall neutral which makes the PBC a consistent choice. Differently to most works dealing with long range potentials, we have not employed here the conventional Ewald summation technique (EST). The electrostatic energy has been calculated by a direct sum instead.⁶ In this way we have avoided the introduction of fictitious additional parameters that EST would have required with little or no benefit in terms of convergence speed, as preliminary tests have shown.

^{a)}Electronic mail: juerg.hulliger@iac.unibe.ch

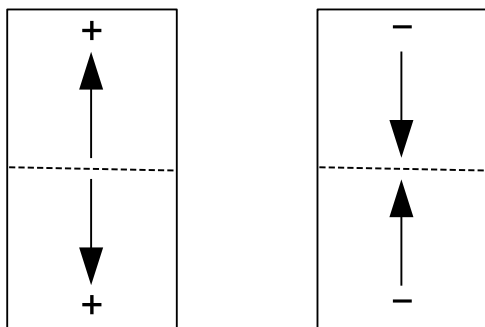


FIG. 1. Schematic representation of bi-polar states. The system exhibits two domains of opposite average polarization.¹

The only degree of freedom of the molecules is a 180° rigid rotation around the axis orthogonal to the molecule through its axis 2. This allows us to introduce an order parameter which can only assume the two values 1 or -1, depending on the two possible molecule orientations, similarly to a spin variable in the Ising model. Specifically, we define an order parameter $P = \hat{e}_1 \cdot \hat{e}_p$, where \hat{e}_p is the unit vector pointing from the N atom (minus partial charge) to the Br atom (plus partial charge) and \hat{e}_1 is the unit vector in the x direction (see Fig. 2).

A state of the system is defined by the N values of the $\{P_i\}$, $i = \{1, \dots, N\}$, i.e., by a point in the N -dimensional configuration space Ω^N . An initial configuration $\{P_i^0\}$ is generated by randomly assigning ± 1 values to the P_i s. Figure 2 shows a typical realization of the initial configuration obtained with this procedure.

An elementary MC step consists of flipping a randomly selected molecule. The new configuration so generated is then accepted or rejected, according to the standard importance

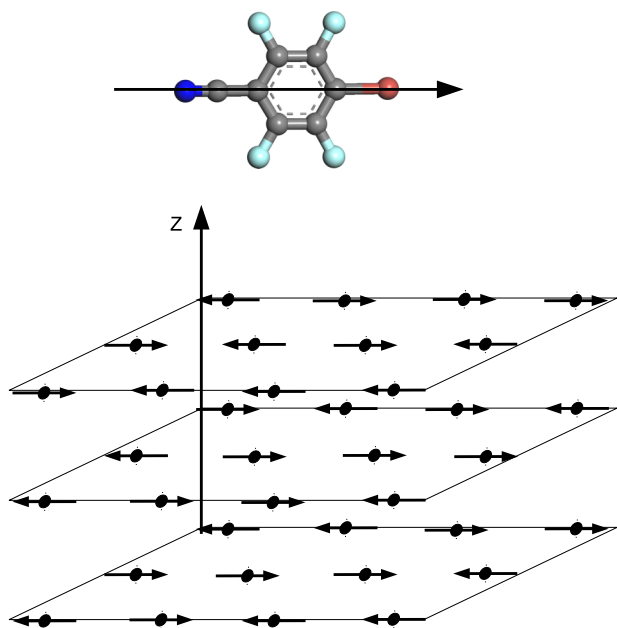


FIG. 2. Top: diagram of the BTfBN molecule with the order parameter axis. Bottom: Example of initial configuration of randomly oriented molecules on a cubic regular lattice. The solid points are pivots for molecular flipping. Chains of molecules are aligned along the x-axis.

sampling Monte Carlo method,⁷ performed in the canonical ensemble, at absolute temperature T . The MC dynamics is defined by a sequence of N_{stp} of such elementary steps. Before starting to sample the order parameter, a certain number of MC steps N_{eq} are performed to reach equilibrium. In order to generate reasonably statistical independent samples, the order parameter has been stored at intervals of 1000 MC steps. In an effort to explore a meaningful region of Ω^N , a number N_{run} of simulations have been performed starting from different and statistical independent initial configurations. This procedure has also the advantage to reduce the statistical errors over the averaged quantities in a more efficient way. We recall, indeed, that this error scales as $N_{\text{stp}}^{-1/2}$ only. For each MC run, the average and the standard error of the sampled order parameter have been calculated. These latter errors have been used to generate the weights of the overall average $\langle P \rangle$.

Simulations have been performed at a temperature of 25 °C (298.15 K), at different inter-molecular distances and system sizes, typically keeping $d_x = d_y = d_z \equiv d$ and $N_y = N_z \equiv N_{\perp}$. The typical chain used contains $N_x = 21$ molecules. We have performed three main sets of simulations: one at fixed system size $N_{\perp} = 11$ varying d in the range 3.5 to 12 (in lattice units); one at fixed inter-molecular distance $d = 5$ and N_{\perp} in the range 1 to 11; and one at $N_{\perp} = 11$, $d = 4$, varying the chain length N_x from 3 to 21 molecules. In the attempt to keep the notation as light as possible in the following, we will refer to the system size as $N_x \times N_y \times N_z$. The largest system simulated contains 2541 molecules or 33 033 atoms. Such a number of molecules is compatible with what we know about the critical size of real nuclei.⁸

It is well known that the combination of PBC and long range interactions may produce artifacts due to the unavoidable finite size of the system. Particular care has been devoted to choose systems big enough to minimize finite size effects. As an *a posteriori* verification, it turns out that all characteristic lengths obtained in our study are over one order of magnitude smaller than the system size.

III. MONTE CARLO RESULTS

A. Long- vs. short-range effects

In a previous work,⁵ we have proven that the average order parameter of a one-dimensional lattice system with next-neighbor (NN) interactions shows, within the *dipole-quadrupole* approximation, a simple exponential behavior of the form

$$\langle P_{mn} \rangle(x) = a[\exp((x-L)b) - \exp((1-x)b)], \quad (3)$$

where L is the chain length, x is the distance inside the chain, and a and $b < 0$ are some constants (with respect to x). This behavior has also been found in three-dimensional lattice systems by MC simulations.⁹

The most striking effect of the long range interaction is the deviation from the exponential behavior of the average order parameter $\langle P \rangle$ as displayed in Fig. 3. Here the data of a system of size $21 \times 11 \times 11$ are compared with a same sized system with next neighbor interactions only. This means that, in this latter system, the potential energy at a distance larger

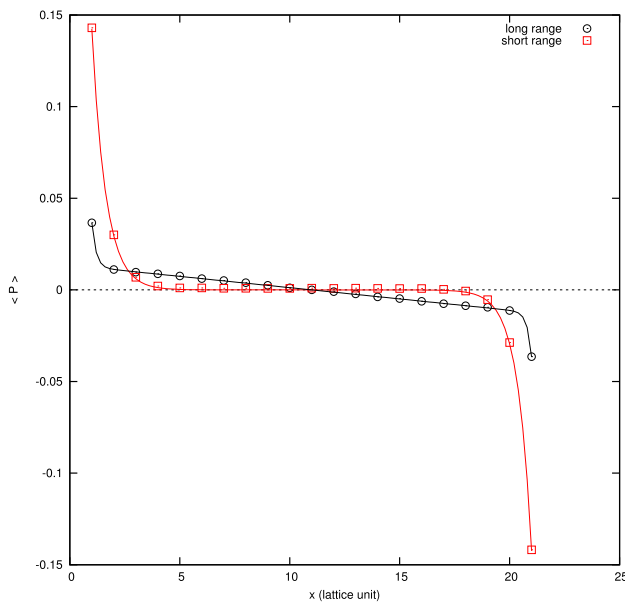


FIG. 3. Long range effect on $\langle P \rangle(x)$ as viewed by comparing the curves of systems with next-neighbor interactions only, and with full interactions. Full lines are fits of functions given by Eq. (4). Data are from simulations of a 11×11 system with $N_x = 21$, and $d = 5$.

than one lattice constant is cut off. At short distances, i.e., near the system surface with FBC, the exponential behavior of $\langle P \rangle$ is preserved over a very short length scale of the order of 1-3 molecule lengths depending on the strength of the interactions. A very narrow crossover region is then entered followed by a linear non-zero regime which extends all the way inside the chains through the specular crossover region next to the opposite surface. The occurrence of this crossover is the fingerprint of the long range interactions and has already been observed in the literature, for instance in charged polymer chains.¹⁰⁻¹²

In order to analyze the data in a more quantitative way we need to define a reasonable fit model. The simplest way to

account for the linear regime is to add a first order polynomial (P1) to Eq. (3). In the following we will prove that the function (EP1) given by

$$f(x) = a[\exp((x-L)b) - \exp((1-x)b)] + c \left(x - \frac{L+1}{2} \right), \quad (4)$$

with the conditions

$$b > 0, c \leq 0, \lim_{L \rightarrow \infty} a(L) = 0, \lim_{L \rightarrow \infty} Lc(L) = 0, |f(x)| \leq 1,$$

where a , b , and c are the fitting parameters, can satisfactorily be fitted to all MC data. We stress that besides b^{-1} , which determines the fast decay range, $f(x)$ in Eq. (4) contains the additional characteristic length c^{-1} , which ultimately controls the slow decay regime. Note also the odd nature of $f(x)$ which reflects the symmetry of the system, i.e., the charge neutrality.

The parameter c can be interpreted as a first order correction to $\langle P_{nn} \rangle(x)$ in Eq. (3). To show this, let us expand the exponential in Eq. (4) in a Taylor series to get

$$\begin{aligned} f(x) &= a \sum_{n=0}^{\infty} \left[\frac{(x-L)^n b^n}{n!} - \frac{(1-x)^n b^n}{n!} \right] + c \left(x - \frac{L+1}{2} \right) \\ &= a' + b'x \\ &\quad + a \sum_{n=2}^{\infty} \left[\left(\exp(-bL) + (-1)^n \exp(b) \right) \frac{(xb)^n}{n!} \right], \end{aligned} \quad (5)$$

where

$$\begin{aligned} a' &= a(\exp(-bL) - \exp(b)) - c \frac{L+1}{2}, \\ b' &= ab(\exp(-bL) + \exp(b)) + c. \end{aligned} \quad (6)$$

Thus, the new first order characteristic length b' contains the additional contribute c .

Finally, we notice that the fit parameters a , b , and c depend, in general, on the system size. Strong indications suggest a scaling behavior of the data (see below). Of course, such symmetry should also be reflected into the fit parameters

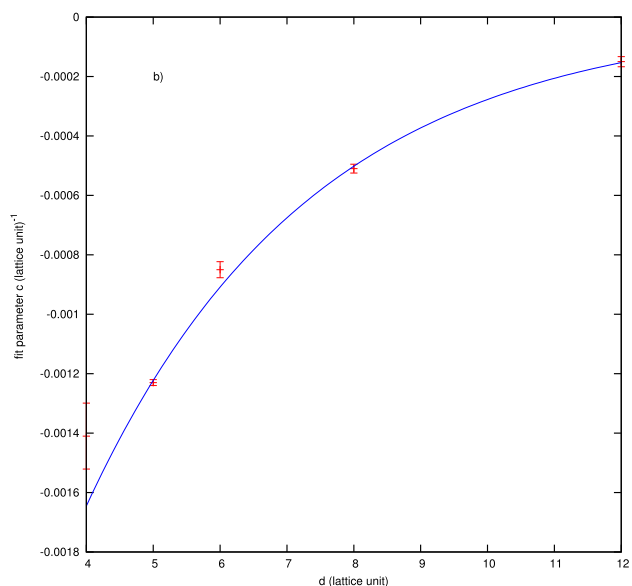
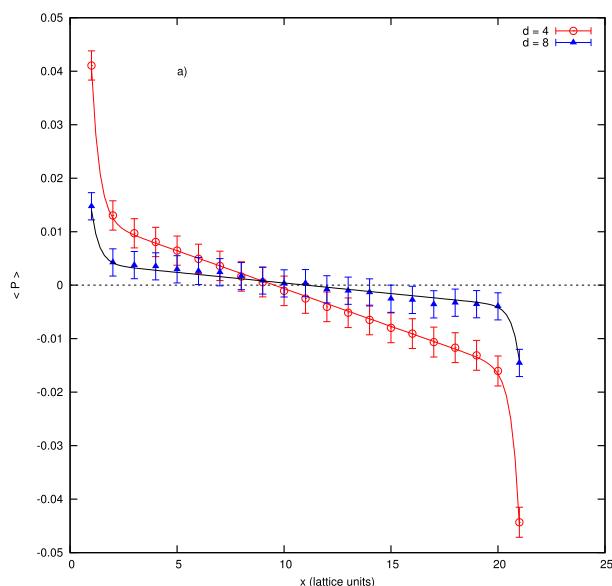


FIG. 4. (a) Example of $\langle P \rangle$ vs. inter-molecular distance inside a chain x . Data refer to simulations at $d = 4$ and $d = 8$, $N_{\perp} = 11$. Full lines are fits with EP1 functions given by Eq. (4). (b) Fit parameter c vs. d for $N_{\perp} = 11$. Full line is a fit with an exponential function. For both pictures are $N_x = 21$.

by requiring, for instance, to be a homogeneous function of the system size.

B. Effects of inter-molecular interactions

The strength of the inter-molecular interactions can be varied by modifying the distance d between molecules. We have performed simulations at $d = 4, 5, 6, 8, 10, 12$, and $N_x = 21$, $N_\perp = 11$. Figure 4 shows the average order parameter vs. x . As expected, on decreasing the inter-molecular distance on the chains, i.e., increasing the strength of the interactions, the overall ordering is enhanced. To analyze this point more in detail we have plotted in Fig. 4(b) the fit parameter c vs. d . We recall that c^{-1} is the characteristic length of the slow polarization decay regime, providing information about

the long range ordering inside the system. The function $c(d)$ can be approximated by an exponential, as the fit (full line) in Fig. 4(b) demonstrates. Although the building of a long range ordering is an evident effect of the interactions, the variation of such ordering appears to be dictated by the magnitude of the inter-molecular distance with respect to the further characteristic length entering the exponential function.

C. Surface charge distribution

The other important quantity to analyze is the average order parameter on the free surfaces $P_s = \langle P(x_0) \rangle$, where $x_0 = \{1, N_x\}$, as it is proportional to the surface charge density σ (at least in a dipolar approximation).^{13,14} Accordingly to the

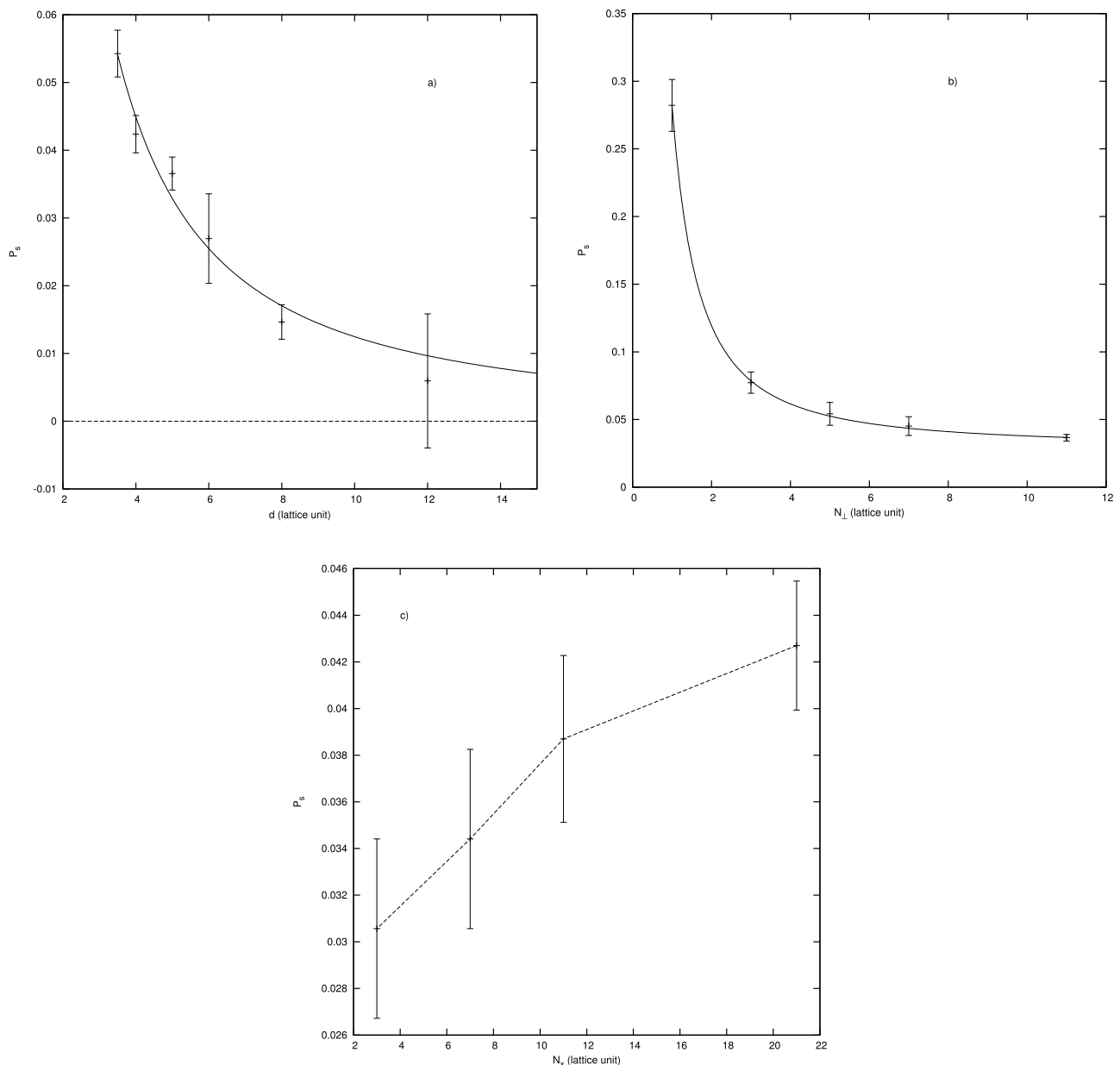


FIG. 5. (a) Surface charge density ($\propto P_s$) vs. inter-molecular distance for system with $d = 5$ and $N_\perp = 11$. (b) Surface charge density vs. planar size N_\perp , with $d = 5$ and $N_x = 21$. Full lines are power law fits. (c) Surface charge density vs. number of molecules in a chain N_x with $d = 4$ and $N_\perp = 11$. The broken line is just a line connecting point for eye guidance.

general approach of this work, we have analyzed the behavior of P_s vs. d , N_\perp , and N_x .

Figure 5(a) shows the decay of P_s with the inter-molecular distance as the result of decreasing the electrostatic interactions, as already seen in Subsection III B. We have found that such decay follows very closely a power law of the kind $\sigma(d) \sim d^{-\beta}$ with $\beta = 1.4 \pm 0.1$. The existence of a scaling law with a homogeneous function of the distance suggests the possibility of a more general symmetry invariance. We will consider this point more in detail in Subsection III D.

The plot of P_s vs. N_\perp (Fig. 5(b)) also shows a decay due to the different ordering stemming from the lateral interactions which favor a different alignment of the molecules. The order parameter $P_s(N_\perp)$ can again be fitted by a power law of the form $P_s(N_\perp) \sim k_1 x^\delta$, with $\delta < 0$. If this would be the correct scaling, the alignment would be completely destroyed and the surface polarization then disappears in the limit of an infinite system. To rationalize this, let us consider that the lateral interactions between adjacent chains decrease the ordering, i.e., the polarization. For a D -dimensional ($D > 2$) system the total number of chains goes as $N_\perp^{(D-2)}$, thus yielding a significant decrease (possibly exponentially) in the net polarization as D increases. If we assume the existence of a space critical dimension D_c such that for dimensions $D > D_c$, in the limit $N_\perp \rightarrow \infty$, the scale invariance is rigorously fulfilled then the polarization vanishes. Our MC data cannot assess if this critical dimension is three or higher and should be further investigated.

Figure 5(c) displays the dependence of P_s on the number of molecules in a chain. The monotonic increasing behavior is likely due to two synergic effects: one is the increased interactions between molecules that tend to order in the same directions on both sides of the chains. The second is caused by the fact that the longer the chain the more distant are the molecules near the free planes and, consequently, their mutual interaction is lowered. Since this interaction

is, from a stand point of the ordering, destructive, a net polarization increase is observed. Of course, at some point $N_x \gg 1$ the curve in Fig. 5(c) should reach a plateau. Our data are, however, still far away from this asymptotic behavior and, as a matter of fact, simulations in this regime are unfeasible. One reasonable speculation could be that still a characteristic exponent might be present. In this case the function $P_s(N_x)$ could be represented, for instance, by the ratio of two powers of N_x with the same exponent, thus having the same order of infinity when $N_x \rightarrow \infty$, i.e., $P_s(N_x) \sim N_x^\gamma / (N_x^\gamma + \text{const.})$, but again our data are inadequate for such an analysis.

D. Effects of system size

In order to accomplish a systematic study on how the system size affects polarity formation in seeds, we have performed simulations at different values of N_\perp ranging from 3 to 11, at fixed inter-molecular distance $d = 5$ and $N_x = 21$. Example of results for $\langle P \rangle(x)$ is reported in Fig. 6. The existence of a bi-polar state is clearly demonstrated by all sets of data.

Although the functional behavior of the order parameter is only slightly affected by the system size, its magnitude shows a significant decrease as N_\perp increases. The effect is particularly pronounced in the inset where the data are compared with a limiting case, namely a single chain in two dimensions. The building up of an ordered structure appears, therefore, the result of a trade off between competing molecular alignment in the system to reach a free energy minimum state. In other words, one can note that, what is preserved is the energy favorable ordering peculiar to the state at $T = 0$, where molecules belonging to a single chain tend to align in the same direction whereas parallel chains tend to be oppositely aligned. As a result, the presence of more chains, as realized by increasing N_\perp , together with the long range character of the Coulomb interactions acts to decrease the ordering.

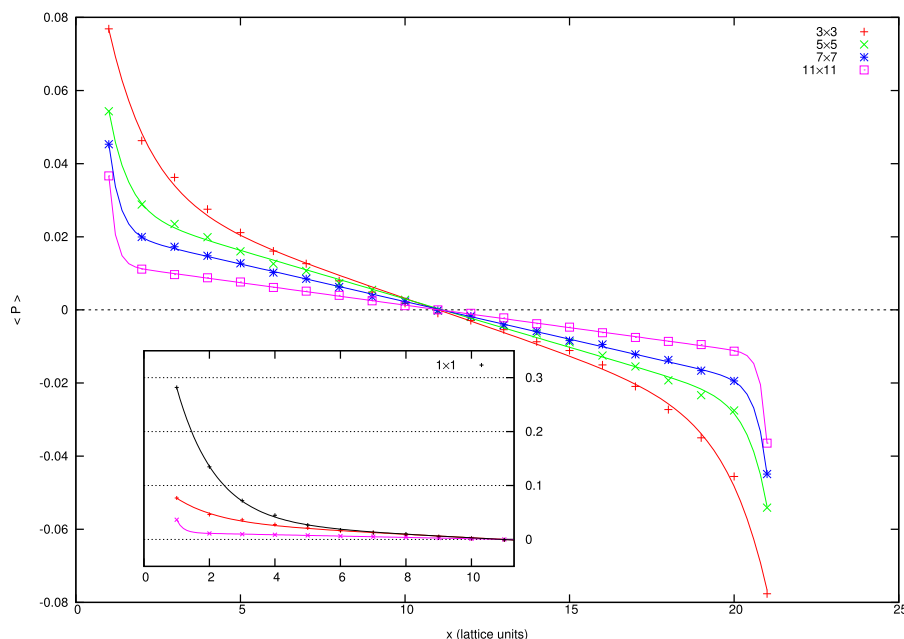


FIG. 6. Example of $\langle P \rangle$ vs. longitudinal distance x for different system sizes: $N_\perp = 11 \times 11$, 7×7 , 5×5 , and 3×3 . Inset comparison of the previous data with a 1×1 system, i.e., with a two-dimensional one. Data refer to simulations at $d = 4$ and $d = 8$. Full lines are fits with EP1 functions given by Eq. (4).

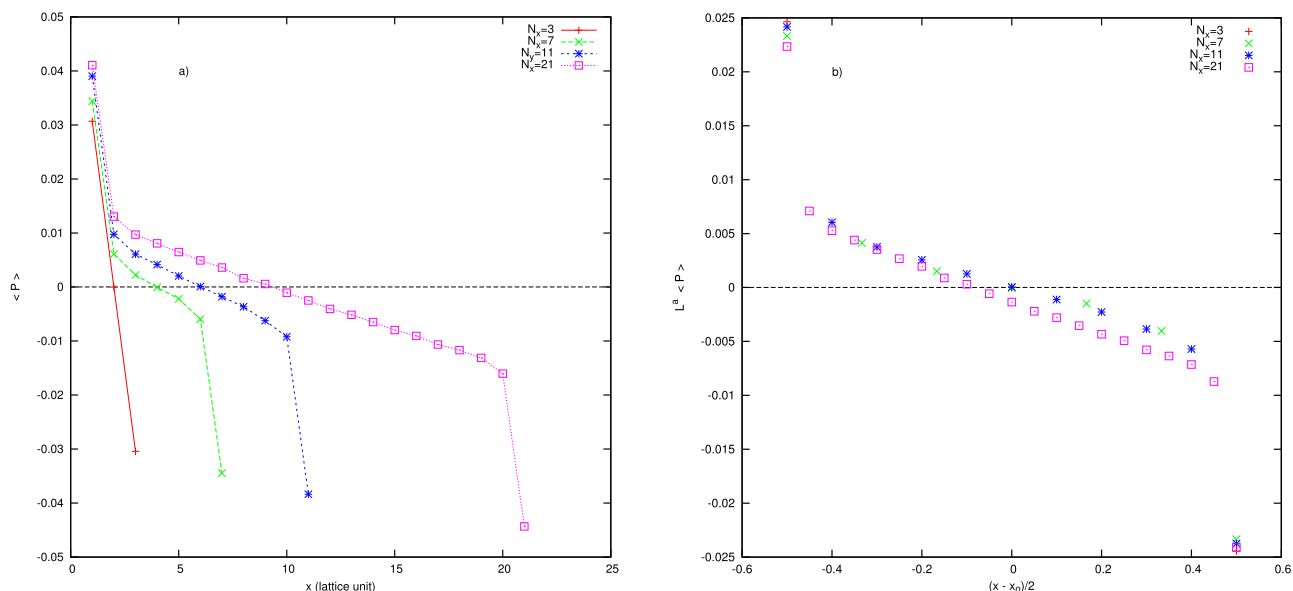


FIG. 7. (a) Average order parameter vs. x for four different chain lengths. (b) Data collapse after rescaling showing the scale invariance of the order parameter. The scaling exponent is $\lambda \simeq -0.2$, and $x_0 = (N_x + 1)/2$.

E. Effects of chain length

The effects of the chain length on the order parameter are particularly interesting. Figure 7(a) shows the data for $\langle P \rangle(x, N_x)$ for $N_x = 3, 7, 11, 21$. The plot suggests that the data, if properly re-scaled, may collapse on a single master curve. Assuming, for instance,

$$\langle P \rangle(x, N_x) = L^\lambda f(t/L) \quad t = x - \frac{N_x + 1}{2}, \quad (7)$$

the data collapse for $\lambda \simeq -0.2$, as Fig. 7(b) demonstrates. Interestingly we observe evidence of scale invariance in the system at the length scale accessible by the simulations.

IV. CONCLUSION

The formation of a bi-polar state on a lattice of polar molecules has been reproduced by MC simulations. Simulations have been performed at different inter-molecular distances resulting in different interaction strengths, and at different system sizes large enough to avoid artifacts due to the simultaneous presence of long range forces and periodic boundary conditions.

The departure from the exponential behavior of the average order parameter into a slower functional decay is the fingerprint of the long range interactions and has been observed at all length scale explored. This represents one significant step ahead of earlier work which considered short range interactions only. As a result, a single characteristic length is no longer sufficient to describe the orientational correlation of distant molecules, but at a first order approximation, at least two are required for a meaningful analysis. To account for this new feature, a semi-empirical fit model has been introduced by adding a polynomial to the exponential decay peculiar to the short range interactions. On the contrary the analysis of

the dependence on the chain length suggests the order parameter to be scale invariant with no characteristic length.

As a general result, the mechanism of ordering resembles that of free energy minimization at low temperatures with parallel alignments of molecules along the chain and anti-parallel in the lateral directions. As a result, this latter alignment acts to decrease the net polarization on the free surfaces of the system. The effect is, of course, larger at higher spatial dimension since the number of chains is significantly increased, alongside with the long range influence of the Coulomb potential. To setup a theoretical framework for further investigation we have speculated on the existence of a critical spatial dimension above it and in limit of infinite systems, the order parameter becomes scale invariant with zero net surface polarization.

In agreement with earlier work assuming just short range interactions, the introduction of long range interactions preserves the general picture of a bi-polar state as the *true* statistical state of such a system. The next step would be the exploration of seed formation by molecular dynamics simulations under full rotational and translational freedom conditions.

ACKNOWLEDGMENTS

The support of the SNF, Project No. 200020_159231, is gratefully acknowledged. We thank Mrs. Khadidja Brahimi for the Gaussian 09 calculations.

¹J. Hulliger, T. Wüst, and M. Rech, *Z. Kristallogr. - Cryst. Mater.* **228**, 607 (2013).

²M. J. Frisch *et al.*, GAUSSIAN 09, Revision D.01, Gaussian, Inc., Wallingford, CT, 2009.

³H. A. Lorentz, *Ann. Phys.* **248**, 127 (1881).

⁴D. Berthelot, *C. R. Acad. Sci. Hebd. Seances* **126**, 1703 (1898).

⁵L. Cannavacciuolo and J. Hulliger, *Symmetry* **8**, 10 (2016).

- ⁶M. P. Allen and D. J. Tildesley, *Computer Simulation of Liquids* (Clarendon Press, 1996).
- ⁷N. Metropolis, A. W. Rosenbluth, M. N. Rosenbluth, A. H. Teller, and E. Teller, *J. Chem. Phys.* **21**, 1087 (1953).
- ⁸D. Hurle, *Handbook of Crystal Growth. Vol. 1: Fundamentals* (North-Holland, 1993).
- ⁹J. Hulliger, T. Wüst, K. Brahimi, M. Burgener, and H. Aboulfadl, *New J. Chem.* **37**, 2229 (2013).
- ¹⁰L. Cannavacciuolo and J. S. Pedersen, *J. Chem. Phys.* **117**, 8973 (2002); **120**, 8862 (2004).
- ¹¹T. B. Liverpool and M. Stapper, *Europhys. Lett.* **40**, 485 (1997).
- ¹²U. Micka and K. Kremer, *Europhys. Lett.* **38**, 279 (1997).
- ¹³G. E. Owen, *Introduction to Electromagnetic Theory* (Courier Dover Publications, 2013).
- ¹⁴L. Cannavacciuolo and J. Hulliger, “Polarity formation in crystals: The basics” (unpublished).